ISSN 1063-7834, Physics of the Solid State, 2021, Vol. 63, No. 10, pp. 1760–1766. © Pleiades Publishing, Ltd., 2021.
Russian Text © The Author(s), 2021, published in Fizika Tverdogo Tela, 2021, Vol. 63, No. 10, pp. 1553–1559.

Antiferrodistortive Soft Mode in $PbZr_{0.024}Ti_{0.976}O_3$ Crystal

S. B. Vakhrushev[a], Yu. A. Bronval'd[a, b], K. A. Petrukhno[a, b, *], S. A. Udovenko[a, b], I. N. Leont'ev[c], and A. Bosak[d]

[a] *Ioffe Institute, St. Petersburg, 194021 Russia*
[b] *Peter the Great St. Petersburg Polytechnic University, St. Petersburg, 195251 Russia*
[c] *Southern Federal University, Rostov-on-Don, 344006 Russia*
[d] *Swiss-Norwegian Beamlines at the European Synchrotron Radiation Facility (ESRF), Grenoble, France*
**e-mail: k.a.petroukhno@gmail.com*

Received May 13, 2021; revised May 13, 2021; accepted May 13, 2021

Abstract—Antiferrodistortive (AFD) soft mode at the M point of the Brillouin zone in the $PbZr_{0.024}Ti_{0.976}O_3$ crystal is detected using inelastic scattering of synchrotron radiation. Group-theoretical analysis and calculations of inelastic structural factors made it possible to unambiguously correlate the critical excitation with rotations of oxygen octahedra. The temperature evolution of the soft mode frequency is revealed and it is shown that it obeys the Curie–Weiss law with the Curie temperature of $T_{AFD} = 438 \pm 5$ K, which is close to the ferroelectric Curie temperature of $T_{FE} = 479.5 \pm 5$ K. The frequency of the antiferrodistortive soft mode is less than the frequency of the doubly degenerate acoustic vibration at the M point. Consequently, intermode interaction and anticrossing when deviating from the Brillouin zone boundary are inevitable.

Keywords: ferroelectrics, antiferroelectrics, phase transitions, lattice dynamics, inelastic scattering of synchrotron radiation

DOI: 10.1134/S1063783421100383

INTRODUCTION

In recent years, scientists have been very interested in antiferroelectric (AFE) crystals. This is due to both with the possibilities of their practical application as a basis for the creation of fast electric energy storage devices and electrocaloric cooling devices and with the interesting phenomena of these compounds. Apparently, the most studied AFE materials are lead zirconate $PbZrO_3$ (PZO), solid solutions based on it $PbZr_{1-x}Ti_xO_3$ (PZT) with $x \leq 0.06$, and compounds isomorphic to them, for example, $PbHfO_3$. In the paraelectric phase, all these compounds have a cubic perovskite structure. It should be noted that the phase transition in most of these compounds to the AFE phase occurs through an intermediate ferroelectric (FE) phase [1, 2]. In single crystals of pure PZO, the FE phase exists in a very narrow temperature range [3, 4], while in lead zirconate ceramics, the intermediate FE phase is observed in a rather wide temperature range [5]. Depending on the concentration of the components in solid solutions and on the external conditions in the compounds of the PZO group, there is a wide variety of structural states including the aforementioned AFE and FE phases [6] and incommensurate structures [7, 8]. The structure of the AFE phases is well studied; there are two order parameters (antiferroelectric parameter characterized by the wave vector q_Σ = (1/4 1/4 0) and the antiferrodistortive parameter characterized by the wave vector q_R = (1/2 1/2 1/2)).

The results of elucidation of the incommensurate structure of $PbHfO_3$ crystal are presented in [8]. At the same time, there is still no unambiguous solution to the structure of the FE phase of PZT with $x \leq 0.06$ despite a large number of works devoted to this problem [9–12]. The structure of these compounds is difficult to identify due to the coexistence of order parameters of different symmetry. If we assume that the transition from the paraelectric phase to the FE phase is an inherent ferroelectric parameter, then the primary order parameter should be considered polarization. However, superstructure reflections at the M point of the Brillouin zone and additional satellite reflections appear in the FE phase [13, 14]. The arising M superstructure cannot be correlated with the antiferrodistortive (AFD) order parameter associated with parallel rotations of oxygen octahedra in neighboring planes, since there is no damping law specific for such an order parameter [10]. Moreover, as was shown in [14], the complex set of satellite reflections does not fit into the pattern of antiphase domains proposed in [10, 15]. One of the most effective ways to find an answer to the question of the formation of the

FE phase structure is to trace the relevant critical dynamics.

The question of the lattice dynamics of PZO materials has been considered many times. The behavior of the FE soft mode in the center of the Brillouin zone was studied [16]. Dynamic models determining the occurrence of the AFE order parameter are proposed in [17, 18] and the excitations responsible for the incommensurate phase transition are revealed. Much attention was paid to the issue of soft mode at the R point. In a number of theoretical works, it is the softening of the AFD mode that was considered as the main softening that initiates the AFE phase transition. This concept was not confirmed for a pure PZO crystal, and it was shown that the R order parameter arises by the trigger way [17, 18]. At the same time, the authors of [19] revealed the R mode in the $PbHfO_3$ crystal and assumed that it is this mode that is the primary mode. The lattice dynamics in the vicinity of the M point remains poorly studied than the lattice dynamics in the vicinity of the R point. Optical methods do not allow direct investigation of excitations at the boundary of the Brillouin zone. The optimal method for studying oxygen ADF modes is inelastic neutron scattering, but PZT single crystals are too small. In practice, the only way to study phonon dynamics in them is inelastic scattering of X-ray (synchrotron) radiation. Indirect information on the critical dynamics can be obtained from an analysis of the temperature evolution of diffuse scattering. Intense diffuse scattering in the vicinity of the M point in both pure PZO crystal and PZT solid solutions was described in a number of works [20–22]. However, in most cases, measurements were taken at a fixed temperature. In this case, SR scattering had a significantly asymmetric distribution, and the only work, in which diffuse neutron scattering is studied [21], states that the intensity maximum is at the M point, although there is no information on the temperature dependence of this maximum. Damping laws are of fundamental importance for the interpretation of the observed diffuse scattering pattern. A strong diffuse scattering is observed at the points of reciprocal space $(h + 1/2\ k + 1/2\ l)$ at $h \neq k$. The scattering practically disappears at $h = k$. Such selection rules are characteristic of the oxygen AFD mode. The temperature evolution of the diffuse scattering at the M point in $PbZr_{0.993}Ti_{0.007}O_3$ crystal is considered in [22].

J. Hlinka et al. [23] presented the results on studying the lattice dynamics of the $PbZr_{0.475}Ti_{0.525}O_3$ crystal. Special attention was paid to the study of phonon resonances at the M point. When analyzing the data, the oxygen AFD mode was excluded from consideration, apparently on the assumption that its contribution is extremely small due to the relative smallness of the atomic scattering factors of oxygen, in comparison with the atomic scattering factors of lead. However, it should be noted that this argument, which is uniquely important for Bragg scattering, becomes controversial for single-phonon inelastic scattering. The question of the fundamental observability of the oxygen AFD soft mode in experiments on inelastic X-ray scattering is considered below.

In sum, it should be noted that there are no experimental data confirming or refuting the existence of the AFD soft mode at the M point in crystals. It should be noted that the authors of theoretical works devoted to the lattice dynamics of PZO crystal and solid solutions based on it paid very little attention to the behavior of the oxygen mode at the M point. The authors of [24] showed that in the cubic phase of PZO crystal at 0 K, the frequency of the M_3 mode is imaginary and approximately equal to the frequency of the R_{25} mode. The results of an experimental study of the temperature evolution of inelastic SR scattering in $PbZr_{0.993}Ti_{0.007}O_3$ crystal with wave vectors along the Σ line $(qq0)$ including the M point are presented in [25]. The scattering intensity in the region of low transferred energies increases with approaching the M point, although the line form and issues of mode softening have not been analyzed in detail.

To answer the question about the frequency of the oxygen AFD mode and its temperature evolution, we studied inelastic SR scattering in a single crystal $PbZr_{0.024}Ti_{0.976}O_3$ (PZT2.4). There are two successive phase transitions in the crystal. They are (1) the transition from paraelectric phase to ferroelectric phase at $T_1 \approx 520$ K accompanied by the formation of an M superstructure and the transition from FE phase to AFE phase at $T_2 \approx 420$ K. The measurements were carried out in the paraelectric phase at the temperature range from 550 K to 700 K.

FORMULATION OF THE PROBLEM

Oxygen Soft Mode in PZT Crystals

As a rule, it is difficult to reliably reveal the contribution of light elements to X-ray scattering with heavy elements. Indeed, when we talk about Bragg scattering, the partial contribution of the elements that make up the substance to the total scattering intensity is proportional to the value of the atomic scattering factor f, i.e., to the atomic number Z in the first approximation. In the case of inelastic scattering, the dependence on f remains basically the same, but there exist an additional dependence on the amplitude of atomic displacements. The scattering function for single-phonon inelastic scattering of X-ray radiation $S_j(\mathbf{Q}, \omega)$ can be written as

$$S_l(\mathbf{Q}, \omega) = [F_j(\mathbf{Q}, \mathbf{q})]^2 G_j(\omega, \omega_j(\mathbf{q}, T)). \qquad (1)$$

Here, j is the number of the phonon mode; $\mathbf{Q}$ is the transferred wave vector; $\hbar\omega$ is the transferred energy; $\mathbf{q}$ is the reduced wave vector; T is temperature; and $\omega_j(\mathbf{q})$ is the frequency of the phonon with the wave vector **q** belonging to the j mode. The inelastic structure factor is

$$F_j(\mathbf{Q},\mathbf{q}) = \Sigma_l \frac{f_l}{\sqrt{M_l}} \mathbf{Q}\mathbf{e}_l^j(\mathbf{q}) \exp(i\mathbf{Q}\mathbf{r}_l) \exp(-W_l) \\ = \Sigma_l b_l \mathbf{Q}\mathbf{e}_l^j(\mathbf{q}) \exp(i\mathbf{Q}\mathbf{r}_l) \exp(-W_l), \quad (2)$$

where l is the number of atoms in the unit cell; **e** is the eigenvector of displacement; **r** is the position of the atom in the unit cell; f_l is the atomic scattering factor; and M_l is the mass of the lth atom. It is clearly seen that it is possible to introduce the effective scattering amplitude $b_l = f_l/\sqrt{M_l}$. The dynamic response $G_j(\omega, \omega_j(\mathbf{q}, T))$ is described by the expression

$$G_j(\omega, \omega_j(\mathbf{q}, T)) = \left[n(\omega) + \frac{1}{2} \pm \frac{1}{2}\right] \mathrm{Im}(\chi_j(\mathbf{q})), \quad (3)$$

where $n(\omega)$ is the population factor; the plus sign corresponds to processes of the production of a phonon; the minus sign corresponds to processes of the absorption of a phonon; and $\mathrm{Im}(\chi_j(\mathbf{q}))$ is the imaginary part of the generalized susceptibility more simply described by a damped harmonic oscillator

$$\chi_j = 1/(\omega^2 - \omega_j^2 + i\Gamma_j\omega), \quad (4)$$

where Γ_j is the damping constant. In the high-temperature approximation $kT \ll \hbar\omega$, which is usually correct for a soft mode, the energy-integrated dynamic response turns out to be inversely proportional to the square of the phonon frequency

$$\int_{-\infty}^{\infty} G_j(\omega, \omega_j(\mathbf{q}, T)) \propto 1/\omega_j^2. \quad (5)$$

Using the above expressions, it is possible to estimate the oxygen AFD of the soft mode in the PZO-type compound. According to [23], we assume that the main contribution to the doubly degenerate $M_{5'}$ mode comes from the displacements of lead ions. The AFD M_3 mode is purely oxygen. As noted above, we assume that the atomic scattering factors are proportional to the atomic number. Then, we have

$$\frac{b_{\mathrm{O}}^2}{b_{\mathrm{Pb}}^2} \approx \left(\frac{z_{\mathrm{O}}^2}{M_{\mathrm{O}}}\right) \frac{z_{\mathrm{Pb}}^2}{M_{\mathrm{Pb}}} \approx 0.11. \quad (6)$$

Thus, it can be expected that the inelastic structure factor of the AFD mode is not negligible (the exact value depends on the transferred wave vector **Q**). The factor determining the observability of the oxygen mode is the magnitude of the dynamic response. In the general case, the frequencies of vibrations associated with the displacement of heavy atoms turn out to be lower than the frequencies of vibrations associated with the displacement of light atoms. However, a feature of soft modes is a sharp decrease in their frequency as the critical temperature is approached. For example, in the ferroelectric relaxor $Na_{0.5}Bi_{0.5}TiO_3$, in which the ferroelectric and antiferrodistortive modes coexist, the energy of the M_3 mode near the transition temperature from the cubic phase to the tetragonal phase decreases to almost 0.5 meV [27].

Group-Theoretical Analysis and Selection Rules for Inelastic Scattering

We write down the coordinates of the atoms included in the structure.

Pb: (0 0 0); Zr(Ti): (1/2 1/2 1/2); O_1: (1/2 1/2 0); O_2: (1/2 0 1/2); and O_3: (0 1/2 1/2).

The expansion of the mechanical representation into irreducible Brillouin zones at the M point for various ions D_j, where j is the type of ion, is

$$D_{\mathrm{Pb}} = M_{2'} + M_{5'}; \quad D_{\mathrm{Zr(Ti)}} = M_{3'} + M_{5'}; \\ D_{\mathrm{O}} = M_1 + M_2 + M_{2'} + M_3 + M_4 + M_5 + M_{5'}. \quad (7)$$

For irreducible representations, we use the notation from [28]. The irreducible representations M_1, M_2, $M_{2'}$, M_3, $M_{3'}$, and M_4 are one-dimensional and the corresponding phonon modes (which we call according to their irreducible representations) are not degenerate, and the two-dimensional representations M_5 and $M_{5'}$ describe doubly degenerate vibration modes. The eigenvectors of vibrations $M_{2'}$, $M_{3'}$, and M_5 are directed along the Z axis and cannot be observed in the ($hk0$) plane due to the vanishing of the scalar product in formula (2). Purely oxygen modes M_2 and M_3 are extinguished at points ($h + 1/2$, $k + 1/2$, l) when $h = k$ [29]. As noted above, the M_3 mode is associated with the rotation of the oxygen octahedron as a whole and can have a very low frequency, while the M_2 mode is associated with the deformation of the octahedron and, as a rule, has a high frequency [24]; the probability of its observation in an experiment on inelastic X-ray scattering is extremely small. There are no selection rules for modes M_1 and M_4.

EXPERIMENTAL

The PZT2.4 single crystal was grown at the Southern Federal University (Rostov-on-Don, Russian Federation) according to the technique described in [26]. To study inelastic scattering, rod-like samples with a length of about 1 mm and with a rectangular cross section (~50 × 150 μm²) were fabricated. The sample was cut from a larger single crystal, ground, and etched in boiling hydrochloric acid. The measurements were carried out using a spectrometer installed on the ID28 line of the European Synchrotron Radiation Facility (ESRF). Most of the measurements were carried out at a radiation energy of 21.747 keV (Si (11, 11, 11) monochromator, energy resolution is ≈1.7 meV). Heating was carried out with a stream of nitrogen using a Cryostream 700 Plus. The accuracy of maintaining the temperature was ≈1 K. All measure-

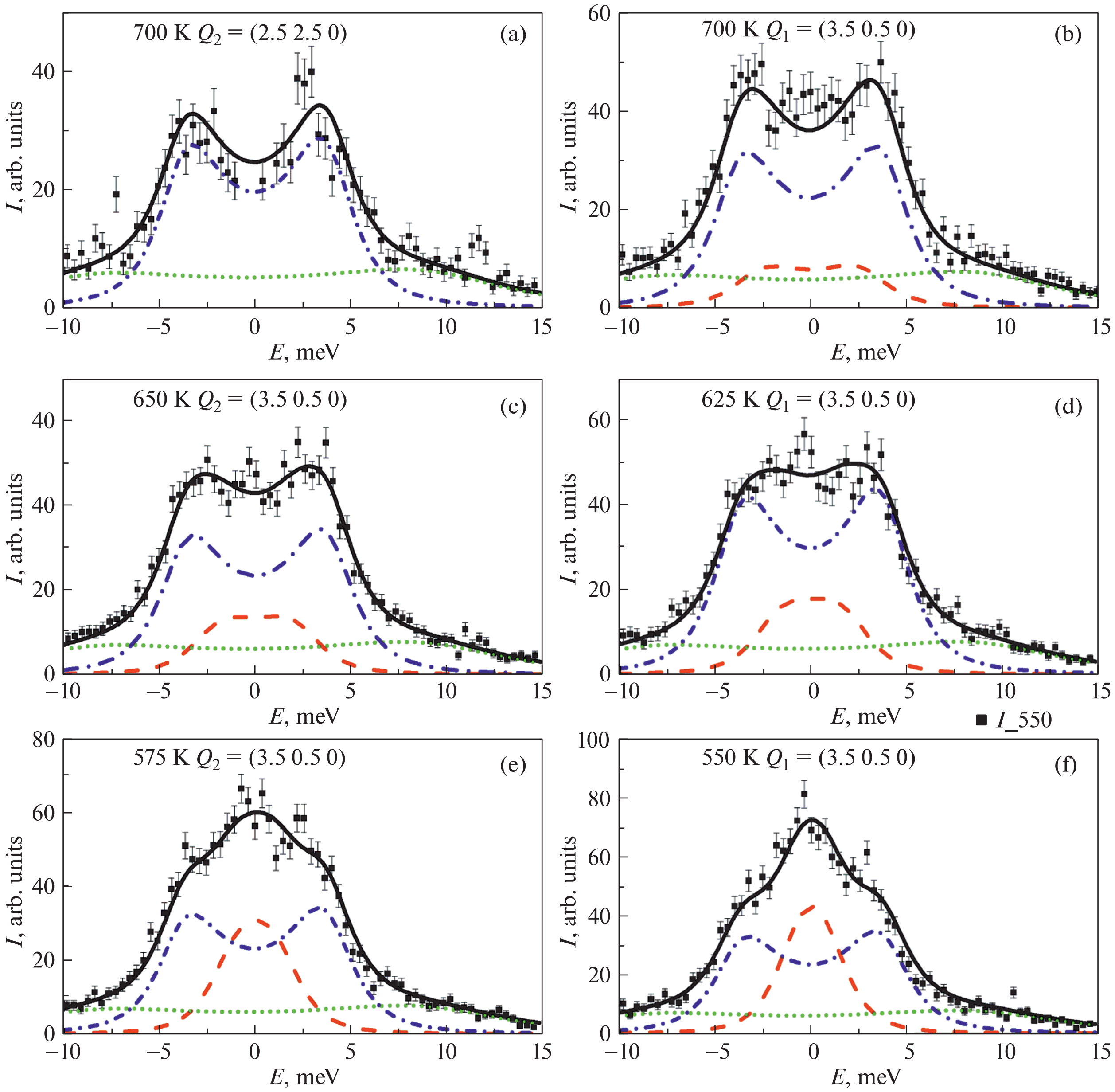

Fig. 1. Temperature evolution of the spectra of inelastic SR scattering at the M point of the Brillouin zone. (a) $Q_2 = (2.5\ 2.5\ 0)$ at 700 K (three points in the center are thrown out); (b), (c), (d), (e), and (f) $Q_1 = (3.5\ 0.5\ 0)$. The total intensity is shown by the solid line; the contributions of the acoustic mode, AFD mode, and optical mode are shown by the dash-dotted line, dashed line, and dotted line, respectively.

ments were carried out in the plane of the reciprocal lattice (*hk*0).

RESULTS AND DISCUSSION

Figure 1 shows the phonon spectra measured at the point of $Q_1 = (3.5\ 0.5\ 0)$ at $T = 700$ K, 650 K, 575 K, and 550 K and at the point of $Q_2 = (2.5\ 2.5\ 0)$ at 700 K. The spectra at the Q_2 point are similar to those described in [23] for morphotropic PZT crystal and agree with data from [22] for $PbZr_{0.993}Ti_{0.007}O_3$ crystal. The low-frequency component with a maximum near 4 meV is obviously associated with the doubly degenerate acoustic mode $M_{5'}^{A}$ (merging of the transverse and longitudinal acoustic dispersion curves at the zone boundary), and the high-frequency component with a maximum near 10 meV is due to the doubly degenerate optical mode with the $M_{5'}^{O}$ symmetry. The spectrum at the Q_1 point at 700 K differs little from the spectrum at the Q_2 point. However, an additional low-energy component is clearly revealed as the temperature decreases and the phase transition to the FE phase approaches. This low-frequency contribution cannot be due to the $M_{2'}$ mode, since it cannot be observed in the ($hk0$) plane, as noted above. Comparison with theoretical calculations allows one to correlate the low-frequency scattering at the Q_1 point with the M_3 AFD mode.

The experimentally observed spectra at the Q_1 point are poorly resolved, which gives great inaccuracy when approximated by a sum of independent phonon resonances (3). To significantly improve the unambiguity of the results, we use two approximations. We assume that the frequencies of the acoustic $M_{5'}^A$ vibrations and optical $M_{5'}^O$ vibrations are independent of temperature. For the $M_{5'}^A$ vibration, this fact follows from the results obtained for pure lead zirconate [17] and the $PbZr_{0.985}Ti_{0.015}O_3$ solid solution [22].

We also assume that $M_{5'}^A$ is almost entirely related to the displacements of the lead ion. First of all, this assumption is supported by the calculation results for pure $PbZrO_3$ crystal using the methods of molecular dynamics [20].

The measured spectra are described as the sum of four phonon resonances

$$I = A(T)[[F_{A1}^2(\mathbf{Q})G_A + F_{A2}^2(Q)G_A] + F_{\mathrm{AFD}}^2(\mathbf{Q})G_{\mathrm{AFG}}(T) + F_{\mathrm{O}}^2(\mathbf{Q})G_{\mathrm{O}}], \tag{8}$$

where $A(T)$ is the temperature-dependent scale factor; G_A, G_{AFD}, and G_{O} are the dynamic responses; and F_{A1}^2, F_{A2}^2, F_{AFD}^2, and F_{O}^2 are inelastic structural factors for doubly degenerate acoustic mode, antiferrodistortive mode, and optical mode. The inelastic structural factors for the acoustic mode and AFD mode were calculated using formula (2). The eigenvector of the AFD mode is completely determined by the one-dimensional irreducible representation M_3, which is included in the expansion of the mechanical representation once, and is $e_{\mathrm{AFD}} = e_{\mathrm{AFD}}^{\mathrm{O}_1} \oplus e_{\mathrm{AFD}}^{\mathrm{O}_2} = (100) \oplus (0-10)$ (represented as the direct sum of two vectors related to O_2 and O_3, respectively). The acoustic mode is doubly degenerate and can be represented as the sum of two modes. Any orthonormal pair of vectors in the X–Y plane can be chosen as eigenvectors (taking into account the assumption made about the dominant role of lead displacements). In principle, it is always possible to choose this pair in such a way that the inelastic structure factor has a nonzero value for only one mode, but it would be necessary to unfold the basis for each transferred wave vector. We have chosen the option

$$e_A^1 = (1/\sqrt{2}, -1/\sqrt{2}, 0), \quad e_A^2 = (1/\sqrt{2}, 1/\sqrt{2}, 0).$$

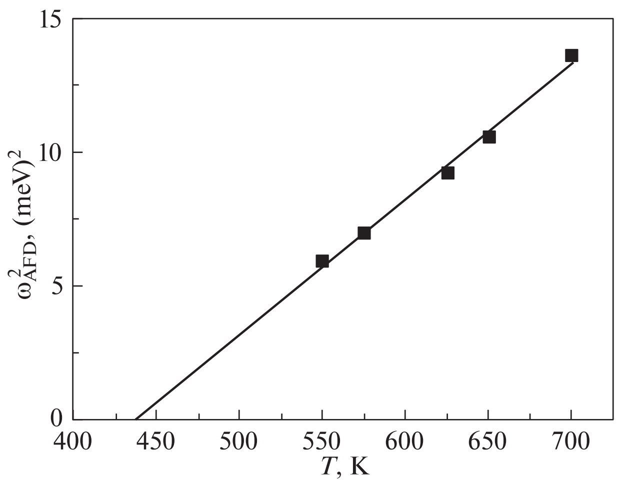

Fig. 2. Temperature dependence of the squared antiferrodistortive mode frequency.

These options allows us to use the script we have written to process the results at arbitrary points of the Σ line $q = (xx0)$ of the Brillouin zone, where the doubly degenerate mode is split into longitudinal mode and transverse mode. The eigenvectors of the optical mode are a linear combination of the PbZr(Ti) and O_3 displacements in the X–Y plane. The relative contributions of these displacements are determined by the details of the interatomic interactions. To date, there are no theoretical calculations describing the lattice dynamics at finite temperatures. Consequently, F_{O}^2 was considered an independent parameter during processing. The frequencies and damping constants of the acoustic and optical modes were assumed to be temperature-independent.

To approximate the data by formula (8), we used the MIGRAD variable metric method [30] from the MINUIT C++ package through the iminuit Python interface. The fitting results are shown by lines in Fig. 1. Figure 1a shows the spectrum measured at 700 K at the point of $Q = (2.5\ 2.5\ 0)$, where it vanishes. All other spectra (Figs. 1b, 1c, 1d, and 1f) were measured at $Q = (3.5\ 0.5\ 0)$. It can be seen that at 700 K the contribution of the AFD mode is very small and could be revealed only due to the simultaneous processing of the spectra at two points and fixing the values of inelastic structural factors calculated using the above eigenvectors. As the temperature decreases and approaches the phase transition point, the frequency of the AFD mode decreases and the peaks associated with the production and annihilation of phonons merge. Starting from the temperature of 625 K, a transition to the overdamped mode occurs, and there is one peak at $\omega = 0$, the width of which is determined by the ratio $\omega_{\mathrm{AFD}}^2/\Gamma_{\mathrm{AFD}}^2$.

Figure 2 shows the temperature dependence of the squared frequency of the AFD mode. It can be seen that it is well described by the Curie–Weiss law $\omega^2_{AFD} \propto (T - T_{AFD})$ with $T_{AFD} = 438 \pm 5$ K. One can pay attention to the fact that the critical temperature in the $PbZr_{0.99}Ti_{0.01}O_3$ compound, which is close in composition, determined from the data of dielectric measurements, $T_{FE} = 479.5$ K [6] is only slightly higher than T_{AFD}. This fact raises the question of the interaction between the AFD mode and the soft mode in the center of the Brillouin zone, which is responsible for the FE phase transition. Obviously, the linear term describing the interaction cannot exist, although the biquadratic term is always allowed. One more important point should be noted. At the M point, the frequency of the oxygen AFD mode turns out to be lower than the frequency of acoustic vibrations. Given that the frequency of the oxygen mode increases rapidly when it deviates from this point (at least in directions other than the line connecting the M points and R points), intermode interaction leading to the anticrossing of the dispersion curves is inevitable. It can be assumed that it is precisely this interaction that is responsible for the fact that the damping laws for the soft mode discovered by us and superstructural reflections at the M point do not coincide (superstructural reflections $(h + 1/2\ k + 1/2\ l)$ are observed for all h, k, and l, while the soft M_3 mode reveals only at $h \neq k$).

One more remark needs to be made. Taking into account the above results, it should be noted that the soft mode revealed in morphotropic PZT crystal is not unambiguously assigned to the $M_{5'}$ mode [23]. Our direct calculations of inelastic structural factors confirm the observability of the oxygen AFD mode and, accordingly, the need to consider its contribution to the observed spectra.

CONCLUSIONS

We measured inelastic scattering of X-ray (synchrotron) radiation and revealed the soft mode at the M point of the Brillouin zone in the PZT2.4 crystal. Analysis of the selection rules and direct calculation of inelastic structural factors made it possible to unambiguously correlate the soft mode with the antiferrodistortive oxygen mode of the M_3 symmetry. The frequency of this mode obeys the Curie–Weiss law with the critical temperature of $T_{AFD} = 438 \pm 5$ K, which is close to the ferroelectric Curie temperature of $T_{FE} = 479.5$ K. Consequently, there is an assumption of a possible interaction between the ferroelectric mode and antiferrodistortive mode. The frequency of the AFD mode at the M point is less than the frequency of the acoustic mode at the M point. Due to the ratio of frequencies, intermode interaction and anticrossing when deviating from the M point (in particular, in the direction of [110]) are inevitable.

FUNDING

This work was supported by the Russian Foundation for Basic Research, project no. 20-02-00724-a.

CONFLICT OF INTEREST

The authors declare that there is no conflict of interest.

REFERENCES

1. Z. Ujma and J. Hańderek, Phys. Status Solidi A **28**, 489 (1975).
2. R. W. Whatmore and A. M. Glazer, J. Phys. C **12**, 1505 (1979).
3. K. Roleder and J. Dee, J. Phys.: Condens. Matter **1**, 1503 (1989).
4. J.-H. Ko, M. Górny, A. Majchrowski, K. Roleder, and A. Bussmann-Holder, Phys. Rev. B **87** (18) (2013).
5. R. Faye, H. Liu, J. M. Kiat, B. Dkhil, and P. E. Janolin, Appl. Phys. Lett. **105**, 162909 (2014).
6. K. Roleder, I. Jankowska-Sumara, G. E. Kugel, M. Maglione, M. D. Fontana, and J. Dec, Phase Trans. **71**, 287 (2006).
7. R. G. Burkovsky, I. Bronwald, D. Andronikova, B. Wehinger, M. Krisch, J. Jacobs, D. Gambetti, K. Roleder, A. Majchrowski, A. V. Filimonov, A. I. Rudskoy, S. B. Vakhrushev, and A. K. Tagantsev, Sci. Rep. 7 (2017).
8. A. Bosak, V. Svitlyk, A. Arakcheeva, R. Burkovsky, V. Diadkin, K. Roleder, and D. Chernyshov, Acta Crystallogr., B **76**, 7 (2020).
9. D. Viehland, J.-F. Li, X. Dai, and Z. Xu, J. Phys. Chem. Solids **57**, 1545 (1996).
10. J. Ricote, D. L. Corker, R. W. Whatmore, S. A. Impey, A. M. Glazer, J. Dec, and K. Roleder, J. Phys.: Condens. Matter **10**, 1767 (1998).
11. D. I. Woodward, J. Knudsen, and I. M. Reaney, Phys. Rev. B **72** (10) (2005).
12. Z. An, H. Yokota, N. Zhang, M. Paściak, J. Fábry, M. Kopecký, J. Kub, G. Zhang, A. M. Glazer, T. R. Welberry, W. Ren, and Z.-G. Ye, Phys. Rev. B **103** (5) (2021).
13. D. Viehland, Phys. Rev. B **52**, 778 (1995).
14. D. A. Andronikova, I. A. Bronwald, N. G. Leontyev, I. N. Leontyev, D. Y. Chernyshov, A. V. Filimonov, and S. B. Vakhrushev, Phys. Solid State **61**, 1772 (2019).
15. S. Watanabe and Y. Koyama, Phys. Rev. B **66** (13) (2002).
16. T. Ostapchuk, J. Petzelt, V. Zelezny, S. Kamba, V. Bovtun, V. Porokhonskyy, A. Pashkin, P. Kuzel, M. Glinchuk, and I. Bykov, J. Phys.: Condens. Matter **13**, 2677 (2001).
17. A. K. Tagantsev, K. Vaideeswaran, S. B. Vakhrushev, A. V. Filimonov, R. G. Burkovsky, A. Shaganov, D. Andronikova, A. I. Rudskoy, A. Q. Baron, H. Uchiyama, D. Chernyshov, A. Bosak, Z. Ujma, K. Roleder, A. Majchrowski, J. H. Ko, and N. Setter, Nat. Commun. **4** (1) (2013).

18. R. G. Burkovsky, A. K. Tagantsev, K. Vaideeswaran, N. Setter, S. B. Vakhrushev, A. V. Filimonov, A. Shaganov, D. Andronikova, A. I. Rudskoy, A. Q. R. Baron, H. Uchiyama, D. Chernyshov, Z. Ujma, K. Roleder, A. Majchrowski, and J.-H. Ko, Phys. Rev. B **90**, 144301 (2014).
19. R. G. Burkovsky, I. Bronwald, D. Andronikova, G. Lityagin, J. Piecha, S.-M. Souliou, A. Majchrowski, A. Filimonov, A. Rudskoy, K. Roleder, A. Bosak, and A. Tagantsev, Phys. Rev. B **100**, 014107 (2019).
20. M. Paściak, T. R. Welberry, A. P. Heerdegen, V. Laguta, T. Ostapchuk, S. Leoni, and J. Hlinka, Phase Trans. **88**, 273 (2014).
21. N. Zhang, M. Paściak, A. M. Glazer, J. Hlinka, M. Gutmann, H. A. Sparkes, T. R. Welberry, A. Majchrowski, K. Roleder, Y. Xie, and Z.-G. Ye, J. Appl. Crystallogr. **48**, 1637 (2015).
22. D. A. Andronikova, I. A. Bronwald, I. N. Leontiev, N. G. Leontiev, D. Y. Chernyshov, A. V. Filimonov, and S. B. Vakhrushev, Ferroelectrics **538**, 65 (2019).
23. J. Hlinka, P. Ondrejkovic, M. Kempa, E. Borissenko, M. Krisch, X. Long, and Z. G. Ye, Phys. Rev. B **83** (14) (2011).
24. P. Ghosez, E. Cockayne, U. V. Waghmare, and K. M. Rabe, Phys. Rev. B **60**, 836 (1999).
25. D. A. Andronikova, I. A. Bronwald, R. G. Burkovsky, I. N. Leontiev, N. G. Leontiev, A. A. Bosak, A. V. Filimonov, and S. B. Vakhrushev, J. Phys.: Conf. Ser. **769**, 012070 (2016).
26. N. Leont'ev, V. G. Smotrakov, and E. G. Fesenko, Izv. Akad. Nauk SSSR, Neorg. Mater. **18**, 449 (1982).
27. P. P. Syrnikov, Sov. Phys. Solid State **25**, 1456 (1983).
28. R. Cowley, Phys. Rev. A **134**, 981 (1964).
29. Yu. Izyumov and N. Chernoplekov, *Neutron Spectroscopy* (Energoatomizdat, Moscow, 1983) [in Russian].
30. F. James and M. Roos, Comput. Phys. Commun. 10, 343 (1975); CERN-DD-75-20.

Translated by I. Obrezanova

SPELL: OK